

Low Complex Image Resizing Algorithm using Fixed-point Integer Transformation

James McAvoy, Ehsan Rahimi and Chris Joslin

Department of Systems and Computer Engineering, Carleton University, 1125 Colonel By Dr., Ottawa, ON, Canada

Keywords: Resizing Algorithm, Image Halving and Doubling, DCT Transformation, Fixed-point Integer Transformation, Subband Approximation, Low-complexity.

Abstract: This paper proposes an efficient image resizing algorithm, including both halving and doubling, in the DCT domain. The proposed image resizing algorithm works on a 4 by 4 DCT block framework with a lower complexity compared to the similar previous methods. Compared to the images that were halved or doubled through the bilinear interpolation, the proposed algorithm produces images with similar or higher PSNR or SSIM values at the significantly lower computational cost. The test results also confirm that our approach improves the current frequency domain resizing algorithms through the fixed-point integer transformation which reduces the computational cost by more than 60% with negligible dB loss.

1 INTRODUCTION

Image resizing algorithms are often required to reduce the memory space or the bandwidth required to store or transmit videos or images. Usually, systems resize videos or images in the spatial domain by decimation or interpolation of pixels; however, it is more beneficial to resize them in the compressed domain, which avoids the high computational overhead associated with decompression and compression operations. Recently, video data is often stored in the compressed format based on blocks of 4×4 discrete cosine transform (DCT) coefficients. Video compression standards such as H.264/AVC (ITU, 2012; ISO, 2012) and H.265/HEVC employ 4×4 fixed-point approximation of the popular DCT to transform frames from the spatial to the frequency domain.

In the early days of developing resizing algorithms in the Discrete Cosine Transform (DCT) domain, researchers devoted effort to image¹ halving and doubling problem. Some of the early contributors in this field were Chang and Messerschmitt (Chang and Messerschmitt, 1995), and Merhav and Bhaskaran (Merhav and Bhaskaran, 1997) who developed resizing algorithms that exploit linear, distributive and unitary transform properties of DCT. Although image quality was similar and often times superior than resizing in

¹Image and video frames will be used interchangeably in this paper.

the spatial domain, the computational complexity was almost same as spatial domain resizing techniques.

Dugad and Ahuja (Dugad and Ahuja, 2001) proposed a simple fast computation algorithm for the image halving and doubling by exploiting the low-frequency DCT coefficients. Later, Mukherjee and Mitra (Mukherjee and Mitra, 2002) proposed some modifications to the Dugad and Ahuja's algorithm that improved the image quality and increased the computational cost. It is worth mentioning that both algorithms use subband approximation of DCT coefficients while performing image resizing operations in the frequency domain. Jiang and Feng (Jiang and Feng, 2002) formulated spatial relationships of the DCT coefficients between a block and sub-blocks. Their approach decomposes and recomposes blocks of DCT coefficients. Mukherjee and Mitra (Mukherjee and Mitra, 2005) also created several resizing algorithms based on decomposition and re-composition combined with subband approximation such as IHAC, IDAD, LMDS, and LMUS algorithms. Depending on the ordering of these operations, one can vary the computational cost and the final image quality for the resizing algorithm.

Among all image resizing algorithms presented recently (Mukherjee and Mitra, 2005; Mukhopadhyay and Mitra, 2004; Nam et al., 2010; Aggarwal and Singh, 2015; Hung and Siu, 2014; Meher et al., 2014), two of these algorithms are the base of others and of

interest to us in this article. The first is the image halving algorithm presented by Mukherjee and Mitra in (Mukherjee and Mitra, 2005), i.e. *Image halving through approximation followed by composition* (IHAC) and the second is its reverse doubling algorithm, *Image doubling through decomposition followed by approximation*. Both of these algorithms include conversion matrix to compose and decompose blocks of DCT coefficients when resizing images in the DCT domain. These matrices consist of entries that are the approximation of irrational numbers. Although conversion matrices contain several zero entries, matrix multiplication with blocks of DCT coefficients contributes most of the overall computational cost; however, both these algorithms have been shown to provide greater efficiency compared to resizing in the spatial domain (Mukherjee and Mitra, 2005; Mukhopadhyay and Mitra, 2004).

This paper aims to enhance the Mukherjee and Mitra image and doubling algorithms by deriving a fixed-point integer approximation of the conversion matrices. Indeed, the proposed fixed-point integer approximation algorithm is very similar to the approach used in H.264/AVC standard body in order to define the default inverse transform process. H.264/AVC deviated from previous video compression standards by employing a 4×4 fixed-point integer transform instead of the popular 8×8 DCT. This way, as reported by Malvar et al. (Hallapuro et al., 2002; Malvar et al., 2003), a reduction in the complexity with the negligible impact on image quality can be achieved.

In this paper, we describe how IHAC and IDDA algorithms that are enhanced by deriving a fixed-point integer conversion matrix from the floating-point conversion matrix, in Section 2. The image quality performance is assessed in Section 3 and then, the computational cost of the proposed algorithms is examined in Section 4.

2 PROPOSED METHOD

Image halving is an operation that takes an image of size $N \times N$ and outputs an image of $N/2 \times N/2$, where image doubling is the inverse operation to resize an image with the resolution of $2N \times 2N$.

Supposing that \mathbf{b} denotes a 8×8 block in the spatial domain containing four adjacent blocks b_k which $k \in \{0, 1, 2, 3\}$ as illustrated in Fig. 1. Therefore, b_k denotes a 4×4 block in the spatial domain whose DCT coefficients are encoded as 4×4 block B_k in the compressed domain. Generally, to half an image one needs to convert four adjacent DCT blocks B_1, B_2, B_3 and B_4 DCT blocks to a single 4×4 DCT block, \mathbf{B}_d .

In Mukherjee and Mitra's IHAC algorithm, four 2×2 adjacent blocks (\hat{B}_k) are derived from the corresponding 4×4 DCT blocks (B_k) using subband approximation and then the 2×2 blocks \hat{B}_k are recomposed to form a single 4×4 block \mathbf{B}_d using the conversion matrix (Mukherjee and Mitra, 2005).

To double an image, Mukherjee and Mitra employed DCT block decomposition (Mukherjee and Mitra, 2005). In the IDDA algorithm, as shown in Fig. 2, a 4×4 DCT block denoted as \mathbf{B} is first decomposed using the conversion matrix to four 2×2 DCT blocks, \hat{B}_k . Then each of these blocks is transformed into a 4×4 DCT block, B_k , by using subband approximation and zero-padding.

To halve this image the IHAC resizing algorithm would contain the following composition step:

$$\begin{aligned} \mathbf{B}_d &= \mathbf{A} \begin{bmatrix} \hat{B}_1^{(2 \times 2)} & \hat{B}_2^{(2 \times 2)} \\ \hat{B}_3^{(2 \times 2)} & \hat{B}_4^{(2 \times 2)} \end{bmatrix} \mathbf{A}^T \\ &= \mathbf{A} \cdot \hat{\mathbf{B}} \cdot \mathbf{A}^T, \end{aligned} \quad (1)$$

Where \cdot denotes matrix multiplication and the conversion matrix, \mathbf{A} , is as:

$$\mathbf{A} = \begin{bmatrix} 1/\sqrt{2} & 0 & 1/\sqrt{2} & 0 \\ 0.6533 & 0.2706 & -0.6533 & 0.2706 \\ 0 & 1/\sqrt{2} & 0 & -1/\sqrt{2} \\ -0.2706 & 0.6533 & 0.2706 & 0.6533 \end{bmatrix}. \quad (2)$$

Note that the rows of \mathbf{A} are orthogonal and have unit norms, which is a necessary condition for an orthogonal block transformation. All the entries in \mathbf{A} require processors to approximate irrational numbers. A fixed-point approximation is equivalent to scaling each row of the conversion matrix, \mathbf{A} , and rounding to the nearest integer. To this end, the conversion matrix is multiplied by 2.5 and then rounded. Therefore, we have \mathbf{C} defined as:

$$\begin{aligned} \mathbf{C} &= \text{round}(2.5 \cdot \mathbf{A}) \\ &= \begin{bmatrix} 2 & 0 & 2 & 0 \\ 2 & 1 & -2 & 1 \\ 0 & 2 & 0 & -2 \\ -1 & 2 & 1 & 2 \end{bmatrix}. \end{aligned} \quad (3)$$

We selected the scaling constant of 2.5 because it was same one that the H.264/AVC designers used to develop their fixed-point approximation of 4-point DCT (Hallapuro et al., 2002; Malvar et al., 2003). To restore the orthonormal property of the original matrix of \mathbf{A} , all the values of c_{ij} in row r are multiplied by $\frac{1}{\sqrt{\sum_j c_{rj}^2}}$:

$$\mathbf{A} = \mathbf{C} \cdot \mathbf{R}, \quad (4)$$

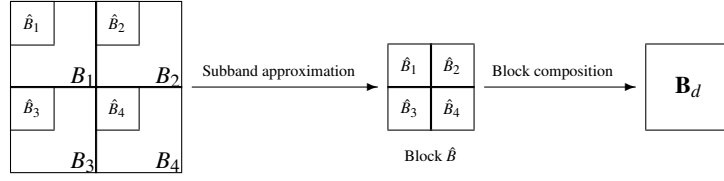


Figure 1: IHAC algorithm-Four 2×2 approximated DCT coefficients of adjacent blocks are composed into one 4×4 DCT block (Mukherjee and Mitra, 2005).

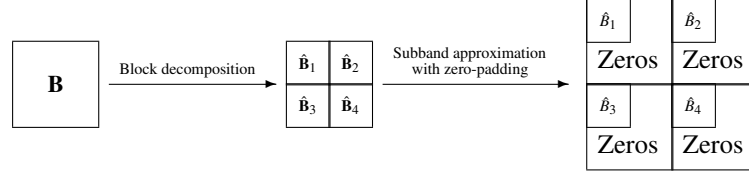


Figure 2: IDDA algorithm-An 4×4 DCT block is decomposed into four $\frac{4}{2} \times \frac{4}{2}$ blocks where each is approximated to an 4×4 DCT block with zero-padding (Mukherjee and Mitra, 2005).

where \mathbf{R} is defined as:

$$\mathbf{R} = \begin{bmatrix} 1/\sqrt{8} & 1/\sqrt{8} & 1/\sqrt{8} & 1/\sqrt{8} \\ 1/\sqrt{10} & 1/\sqrt{10} & 1/\sqrt{10} & 1/\sqrt{10} \\ 1/\sqrt{8} & 1/\sqrt{8} & 1/\sqrt{8} & 1/\sqrt{8} \\ 1/\sqrt{10} & 1/\sqrt{10} & 1/\sqrt{10} & 1/\sqrt{10} \end{bmatrix}, \quad (5)$$

and the operator \bullet denotes an element-by-element multiplication. The two-dimensional transformation in Equation (1) can be rewritten as:

$$\mathbf{B}_d = \mathbf{A} \cdot \hat{\mathbf{B}} \cdot \mathbf{A}^T = [\mathbf{C} \bullet \mathbf{R}] \cdot \hat{\mathbf{B}} \cdot [\mathbf{C}^T \bullet \mathbf{R}^T]. \quad (6)$$

Rearranging to extract the scaling arrays \mathbf{R} :

$$\begin{aligned} \mathbf{B}_d &= [\mathbf{C} \cdot \hat{\mathbf{B}} \cdot \mathbf{C}^T] \bullet [\mathbf{R} \bullet \mathbf{R}^T] \\ &= [\mathbf{C} \cdot \hat{\mathbf{B}} \cdot \mathbf{C}^T] \bullet \mathbf{S}, \end{aligned} \quad (7)$$

Where

$$\begin{aligned} \mathbf{S} &= \mathbf{R} \bullet \mathbf{R}^T \\ &= \begin{bmatrix} 1/8 & 1/\sqrt{80} & 1/8 & 1/\sqrt{80} \\ 1/\sqrt{80} & 1/10 & 1/\sqrt{80} & 1/10 \\ 1/8 & 1/\sqrt{80} & 1/8 & 1/\sqrt{80} \\ 1/\sqrt{80} & 1/10 & 1/\sqrt{80} & 1/10 \end{bmatrix}. \end{aligned} \quad (8)$$

Using the new fixed-point approximation of the conversion matrix \mathbf{C} with its scaling matrix \mathbf{S} , we modified the IHAC algorithm. Fig. 3 outlines our new proposed image halving algorithm that takes advantage of these matrices in the block composition step.

Similarly, we modified the IDDA algorithm in the decomposition step to leverage the fix-point approximation of the conversion matrix with its scaling matrix. Fig 4 displays the outline of our proposed fix-point approximation of the IDDA algorithm (IDDA_{fpa}).

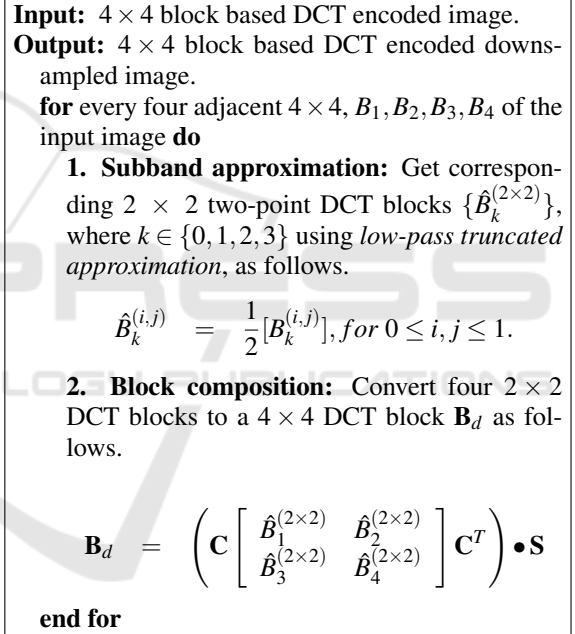


Figure 3: Our proposed resizing algorithm, IHAC_{fpa} , for halving an image based on a 4×4 DCT block framework.

3 QUALITY ASSESSMENT

We developed three experiments to evaluate image quality performance of our proposed fixed-point approximation of the IHAC and IDDA algorithms.

In the first experiment, for each image in the sample set I_{orig} of size $N \times N$ is first spatially downsampled using MATLAB bicubic interpolation with anti-aliasing to an image I_d of size $N/2 \times N/2$. These halved images provided a reference so PSNR can be computed when comparing images produced from va-

Input: 4×4 block based DCT encoded image.
Output: Upsampled image in the compressed domain.
for each 4×4 blocks \mathbf{B} do the following: **do**
1. Block decomposition: Convert the block to four 2×2 DCT blocks as follows.

$$\begin{bmatrix} \hat{\mathbf{B}}_1^{(2 \times 2)} & \hat{\mathbf{B}}_2^{(2 \times 2)} \\ \hat{\mathbf{B}}_3^{(2 \times 2)} & \hat{\mathbf{B}}_4^{(2 \times 2)} \end{bmatrix} = (\mathbf{C}^T \mathbf{B} \mathbf{C}) \bullet \mathbf{S}$$

2. Subband approximation and zero padding: Compute the approximate 4×4 -point DCT coefficients from each of $\hat{\mathbf{B}}_k^{(2 \times 2)}$, where $k \in \{0, 1, 2, 3\}$, *low-pass truncated approximation*.

$$\hat{\mathbf{B}}_k^{(i,j)} = 2 \left[\hat{\mathbf{B}}_k^{(i,j)} \right], \text{ for } 0 \leq i, j \leq 1.$$

Form four 4×4 DCT blocks by zero padding each of them (the high frequency components are assigned to zero).
end for

Figure 4: Our resizing algorithm IDDA_{fpa} for doubling images based on a 4×4 DCT block framework.

rious halving algorithms. The original images I_{orig} in the sample set are raw grayscale (8 bits/pixel) images with a resolution of 512×512 pixels. In all the experiments, we applied `MATLAB dct2` function to transform all the images I_{orig} from the spatial to the DCT domain to represent compressed images formatted as blocks of 4×4 DCT coefficients. We applied the DCT resizing algorithms on the compressed I_{orig} and outputted a compressed halved image. Using `MATLAB idct2`, we transformed these newly compressed halved images back into the spatial domain where we computed an PSNR with the reference halved images. We also compared our proposed halving algorithm with halved images that were resized in the spatial domain by bilinear interpolation, which will be referred as IHS. Tables 1 and 2 show the PSNR and SSIM values computed from comparing the halved images generated from our proposed halving algorithm with IHAC and IHS. As can be seen in these tables, our proposed halving algorithms produces images with slightly lower PSNR or higher SSIM values compared to its floating-point implementation (IHAC), which was expected because of rounding errors associated with integer transforms with scaling. In average, our IHAC_{fpa} algorithm generates images that are 0.13 dB lower PSNR value or 0.0003 lower SSIM value than ones generated from IHAC algorithm; however, images generated from our halving algorithm have 2.27 dB higher quality than the images generated by IHS algorithm.

Table 1: Experiment 1. PSNR values from image halving experiment.

Image	IHS	IHAC	IHAC_{fpa}
Fishing boat	39.94	42.00	41.67
Cameraman	40.47	46.09	45.47
Elaine	45.13	45.87	45.98
Goldhill	42.39	43.63	43.37
House	46.49	50.48	50.92
Jetplane	40.22	44.27	43.99
Lake	39.11	42.80	42.54
Lena	42.00	45.62	45.45
Livingroom	40.06	42.01	41.70
Mandrill	36.54	36.49	36.32
Peppers	42.54	44.94	45.00
Pirate	40.83	43.25	43.07
Walkbridge	37.89	39.74	39.43
Watch	36.69	41.04	40.76
Woman blonde	41.61	42.72	42.60
Woman darkhair	48.73	51.19	51.65
mean(PSNR)	41.29	43.88	43.75

Table 2: Experiment 1. SSIM values from image halving experiment.

Image	IHS	IHAC	IHAC_{fpa}
Fishing boat	0.9920	0.9929	0.9925
Cameraman	0.9950	0.9985	0.9982
Elaine	0.9956	0.9930	0.9929
Goldhill	0.9922	0.9934	0.9931
House	0.9971	0.9992	0.9991
Jetplane	0.9951	0.9976	0.9974
Lake	0.9934	0.9958	0.9956
Lena	0.9947	0.9965	0.9963
Livingroom	0.9913	0.9935	0.9932
Mandrill	0.9823	0.9845	0.9839
Peppers	0.9963	0.9960	0.9959
Pirate	0.9919	0.9949	0.9946
Walkbridge	0.9874	0.9922	0.9917
Watch	0.9952	0.9981	0.9980
Woman blonde	0.9936	0.9937	0.9935
Woman darkhair	0.9979	0.9984	0.9984
mean(SSIM)	0.9932	0.9949	0.9946

Figure 5 show the image "Lena" generated by our IHAC_{fpa} algorithm as well as the ones obtained by IHAC and IHS algorithms. Figure 5a is an image halved through bicubic interpolation with anti-aliasing, which is the reference image so PSNR can be computed. Figure 5b is an image halved by our proposed algorithm, IHAC_{fpa} , with PSNR value of 45.45 dB. Figure 5c was downsampled through floating-point implementation of the IHAC algorithm, which provide a PSNR value of 45.62 dB. Figure 5d was a spatial downsampled image using bilinear interpolation that produced a PSNR value of 42.00 dB.

For the second experiment to evaluate image quality performance of our IDDA_{fpa} algorithm, we first

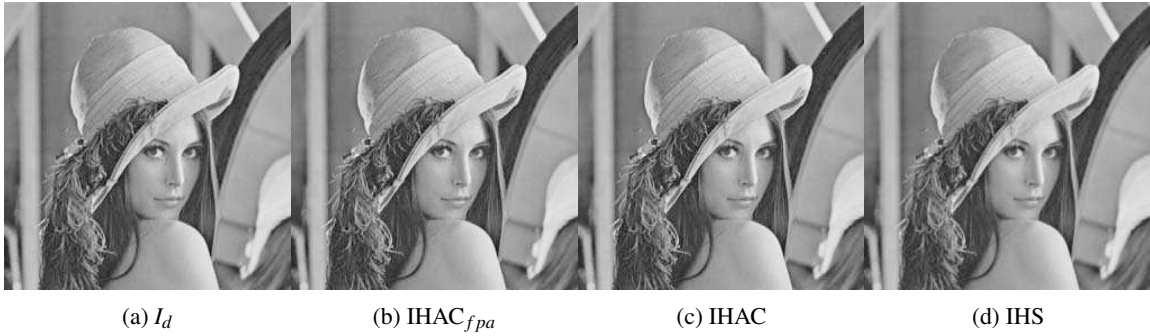


Figure 5: Resultant images downsampled in experiment 1.

spatially downsampled image I_{orig} to create an image I_d that are compressed then upsampled in the DCT domain. We used MATLAB bicubic interpolation with anti-aliasing to halve images in the spatial domain to produce image I_d . Using MATLAB `dct2` function, we transformed the spatially halved image I_d to the DCT domain to represent a compressed image formatted as blocks of 4×4 DCT coefficients. Then we applied the doubling algorithms to resize and output compressed image to the original resolution. We transformed the compressed doubled image back into the spatial domain using MATLAB `idct2` function so a PSNR value can be computed between the upsampled image with the original image I_{orig} . Similar in the first experiment, we doubled the halved image I_d in the spatial domain using bilinear interpolation for comparison, which will be referred as IDS in the paper. Tables 3 and 3 display the results of this experiment. As can be seen by these results, on average our doubling approach created images only 0.07 dB lower than images that were spatially resized; however, in point of SSIM assessment there is about 0.01 improvement. Again, our IDDA_{fpa} algorithm generates images with negligibly lower PSNR and SSIM values compared to the ones generated from IHAC algorithm; although, our IDDA_{fpa} algorithm is considerably less complex as shown in the next section.

In the third experiment, an image is first halved and then doubled. The resulting upsampled image is compared with the original image I_{orig} . We compared the PSNR value computed from images generated from resizing algorithms used in tandem: spatial resizing using IHS-IDS, IHAC-IDDA and our proposed halving and doubling algorithm. The results of this experiment are shown in Tables 5 and 6. As can be seen from the results of this experiment, using our proposed algorithms in tandem provides PSNR values about 0.48 dB lower PSNR value and about 0.0048 lower SSIM value than the IHAC-IDDA pairing but we observed an 1.27 dB PSNR gain or about 0.0476 SSIM gain over the spatial approach imple-

Table 3: Experiment 2. PSNR values from image doubling experiment.

Image	IDS	IDDA	IDDA _{fpa}
Fishing boat	28.94	29.40	29.11
Cameraman	33.21	33.68	32.91
Elaine	32.53	32.75	32.50
Goldhill	30.62	31.03	30.78
House	41.72	41.18	39.66
Jetplane	30.17	30.68	30.28
Lake	29.35	29.77	29.37
Lena	32.69	33.17	32.72
Livingroom	28.59	28.94	28.69
Mandrill	23.05	23.49	23.38
Peppers	31.23	31.62	31.31
Pirate	29.99	30.43	30.14
Walkbridge	26.23	26.70	26.47
Watch	27.11	27.55	27.14
Woman blonde	28.99	29.38	29.19
Woman darkhair	39.84	40.04	39.44
mean(PSNR)	30.89	31.24	30.82

mented using IHS-IDS pairing.

These limited experiments demonstrated to us that our algorithms could produced images equal or better than resizing images in the spatial domain using bilinear interpolation while benefiting from the computational savings derived from our approach. The next section will discuss how computationally efficient our algorithms are.

4 COMPUTATIONAL COST

This section outlines the computational cost of our proposed resizing algorithms. By using a fixed-point approximation of the conversion matrix in our proposed algorithms, we hope to decrease the computational cost. Leveraging fixed-point arithmetic, multiplying or dividing values that are a power of two can be accomplished by binary shift operations. As can be seen in Equation (3), the conversion matrix \mathbf{C} entries are either 0, 1's or 2's. Therefore, matrix multiplica-

Table 4: Experiment 2. SSIM values from image doubling experiment.

Image	IDS	IDDA	IDDA _{fpa}
Fishing boat	0.8274	0.8478	0.8414
Cameraman	0.9551	0.9624	0.9539
Elaine	0.7930	0.8074	0.8038
Goldhill	0.8304	0.8527	0.8475
House	0.9838	0.9837	0.9777
Jetplane	0.9288	0.9373	0.9300
Lake	0.8610	0.8776	0.8705
Lena	0.9021	0.9140	0.9084
Livingroom	0.8194	0.8419	0.8357
Mandrill	0.6576	0.7178	0.7143
Peppers	0.8829	0.8911	0.8832
Pirate	0.8565	0.8774	0.8708
Walkbridge	0.7648	0.8071	0.8009
Watch	0.9383	0.9462	0.9369
Woman blonde	0.8328	0.8526	0.8481
Woman darkhair	0.9590	0.9619	0.9587
mean(SSIM)	0.8621	0.8799	0.8739

Table 5: Experiment 3. PSNR values from image halving followed by image doubling.

Image	IHS IDS	IHAC IDDA	IHAC _{fpa} IDDA _{fpa}
Fishing boat	27.99	29.64	29.37
Cameraman	31.24	33.94	33.16
Elaine	31.89	32.96	32.64
Goldhill	29.81	31.27	31.02
House	38.65	41.73	39.68
Jetplane	29.02	30.88	30.47
Lake	28.15	30.00	29.57
Lena	31.41	33.43	32.92
Livingroom	27.71	29.15	28.93
Mandrill	22.52	23.71	23.62
Peppers	30.35	31.83	31.44
Pirate	29.04	30.66	30.36
Walkbridge	25.43	26.92	26.71
Watch	25.88	27.75	27.33
Woman blonde	28.34	29.59	29.40
Woman darkhair	38.43	40.39	39.48
mean(PNSR)	29.74	31.49	31.01

tions can be carried out *multiplier-free*.

Let assume that n_m and n_a are the total number of multiplications and additions required for the image resizing algorithm, respectively. The IHAC_{fpa} algorithm first performs subband approximation and multiplies each element in the input 4×4 DCT coefficients by half, which can be implemented as a right shift operation; thus, there is no cost. The composition step contains two matrix multiplications by applying the conversion matrix \mathbf{C} on input DCT coeffi-

Table 6: Experiment 3. PSNR values from image halving followed by image doubling.

Image	IHS IDS	IHAC IDDA	IHAC _{fpa} IDDA _{fpa}
Fishing boat	0.7972	0.8591	0.8546
Cameraman	0.9345	0.9648	0.9586
Elaine	0.7775	0.8192	0.8158
Goldhill	0.8003	0.8644	0.8605
House	0.9728	0.9845	0.9797
Jetplane	0.9089	0.9408	0.9359
Lake	0.8335	0.8856	0.8803
Lena	0.8823	0.9200	0.9153
Livingroom	0.7854	0.8537	0.8495
Mandrill	0.6038	0.7455	0.7430
Peppers	0.8678	0.8974	0.8906
Pirate	0.8260	0.8867	0.8817
Walkbridge	0.7156	0.8240	0.8197
Watch	0.9191	0.9497	0.9420
Woman blonde	0.8097	0.8635	0.8596
Woman darkhair	0.9507	0.9644	0.9609
mean(SSIM)	0.8366	0.8890	0.8842

cients twice. Since matrix multiplication with \mathbf{C} can be carried out multiplier-free, only additions count, which there are $n_a = 8$. An element-by-element multiplication is applied with the scaling matrix, \mathbf{S} . As shown in Equation (8), the scaling matrix \mathbf{S} contains four elements equal to $1/8$, which can be implemented as a right shift operation; and twelve elements that need to perform multiplication, thus $n_m = 12$ and $n_a = 0$. Finally, the four 4×4 input DCT blocks represent 64 pixels of the input image. Therefore, on average our method will consume $n_m = 0.1875$ and $n_a = 0.25$ per pixel of the original image.

Similarly, our IDDA_{fpa} algorithm contains two matrix multiplication using the conversion matrix \mathbf{C} . Also, scaling matrix and subband approximation are similar. Therefore, the proposed doubling algorithm requires $n_m = 0.1875$ and $n_a = 0.25$ per pixel of the upsampled image.

Table 7 and 8 compare the computational complexity for the IHAC_{fpa} and IDDA_{fpa} algorithms with other image halving and doubling algorithms, respectively. As shown by these tables, both proposed image halving and doubling algorithms are more efficient than their floating-point implementations. When comparing our proposed halving algorithm, IHAC_{fpa}, with its floating-point implementation, it is 63% more efficient in n_m and 75% in n_a . Regarding doubling algorithm, IDDA_{fpa}, it is 91% more efficient in n_m and 83% in n_a when comparing with its floating-point version, IDDA. When comparing both of our proposed algorithms with spatial resizing, the computational saving is about 85% in n_m and 97% in n_a .

Table 7: Computational complexity of halving algorithms.

ops	IHS	IHAC	IHAC _{fpa}
n_m	1.25	0.5	0.1875
n_a	8.25	1	0.25

Table 8: Computational complexity of doubling algorithms.

ops	IDS	IDDA	IDDA _{fpa}
n_m	1.25	2	0.1875
n_a	8.25	1.5	0.25

5 CONCLUSION

In this paper, we developed a fixed-point approximation of a conversion matrix that is included in IHAC and IDDA resizing algorithms. Matrix multiplications with fixed-point approximation of the conversion matrices are *multiplier-free*, which reduce the computational cost in the proposed resizing algorithms. Images generated by the proposed fixed-point resizing algorithms have PSNR values negligibly lower than PSNR of those images generated by the floating-point implementations; however, the total number of multiplications and additions are substantially decreased. The proposed fixed-point approximation also can be extended so one can resize images by integral or arbitrary factors. Also, there are several resizing algorithms that use conversion matrices for composition and decomposition such as IHCA, IDAD, LMDS and LMUS, which would be good candidates for this approach.

ACKNOWLEDGEMENTS

The authors would like to acknowledge that this research was supported by NSERC Strategic Project Grant: Hi-Fit: High Fidelity Telepresence over Best-Effort Networks.

REFERENCES

- (2012). Advanced video coding for generic audiovisual services.
- (2012). Information technology – coding of audio-visual objects – part 10: Advanced video coding.
- Aggarwal, A. and Singh, C. (2015). Hybrid dct-zernike moments-based approach for image up-sampling. In *2015 Annual IEEE India Conference (INDICON)*, pages 1–6.
- Chang, S.-F. and Messerschmitt, D. G. (1995). Manipulation and compositing of MC-DCT compressed video. *IEEE Journal on Selected Areas in Communications*, 13(1):1–11.
- Dugad, R. and Ahuja, N. (2001). A fast scheme for image size change in the compressed domain. *IEEE Transaction on Circuits and Systems for Video Technology*, 11(4):461–474.
- Hallapuro, A., Karczewicz, M., and Malvar, H. S. (2002). Low-complexity transform and quantization. In *Joint Video Team (JVT) of ISO/IEC MPEG and ITU-VCEG*.
- Hung, K. W. and Siu, W. C. (2014). Novel dct-based image up-sampling using learning-based adaptive k -nn mmse estimation. *IEEE Transactions on Circuits and Systems for Video Technology*, 24(12):2018–2033.
- Jiang, J. and Feng, G. (2002). The spatial relationship of DCT coefficients between a block and its sub-blocks. *IEEE Transaction on Signal Processing*, 50(5):1160–1169.
- Malvar, H. S., Hallapuro, A., Karczewicz, M., and Kerofsky, L. (2003). Low-complexity transform and quantization in H.264/AVC. *IEEE Transaction Circuits and Systems Video Technology*, 13:598–603.
- Meher, P. K., Park, S. Y., Mohanty, B. K., Lim, K. S., and Yeo, C. (2014). Efficient integer dct architectures for hev. *IEEE Transactions on Circuits and Systems for Video Technology*, 24(1):168–178.
- Merhav, N. and Bhaskaran, V. (1997). Fast algorithms for DCT-domain image down-sampling and for inverse motion compensation. *IEEE Transaction on Circuits and Systems for Video Technology*, 7(3):486–476.
- Mukherjee, J. and Mitra, S. K. (2002). Image resizing in the compressed domain using subband DCT. *IEEE Transaction on Circuits and Systems for Video Technology*, 12(7):620–627.
- Mukherjee, J. and Mitra, S. K. (2005). Arbitrary resizing of images in the DCT space. In *IEE Proceeding Vision, Image and Signal Processing*, volume 152, pages 155–164.
- Mukhopadhyay, J. and Mitra, S. (2004). Resizing of images in the DCT space by arbitrary factors. In *Image Processing, 2004. ICIP '04. 2004 International Conference on*, volume 4, pages 2801–2804.
- Nam, H. M., Jeong, J. Y., Byun, K. Y., Kim, J. O., and Ko, S. J. (2010). A complexity scalable h.264 decoder with downsizing capability for mobile devices. *IEEE Transactions on Consumer Electronics*, 56(2):1025–1033.